

RESEARCH LETTER

10.1002/2016GL068273

Key Points:

- Dissolved organic carbon in the deep ocean contains organic surfactants
- Primary marine aerosol can be enriched in refractory dissolved organic carbon
- Atmospheric removal pathway for marine refractory dissolved organic carbon

Supporting Information:

- Supporting Information S1

Correspondence to:

D. J. Kieber,
djkieber@esf.edu

Citation:

Kieber, D. J., W. C. Keene, A. A. Frossard, M. S. Long, J. R. Maben, L. M. Russell, J. D. Kinsey, I. M. B. Tyssebotn, P. K. Quinn, and T. S. Bates (2016), Coupled ocean-atmosphere loss of marine refractory dissolved organic carbon, *Geophys. Res. Lett.*, 43, 2765–2772, doi:10.1002/2016GL068273.

Received 14 FEB 2016

Accepted 1 MAR 2016

Accepted article online 6 MAR 2016

Published online 29 MAR 2016

Coupled ocean-atmosphere loss of marine refractory dissolved organic carbon

David J. Kieber¹, William C. Keene², Amanda A. Frossard^{3,4}, Michael S. Long⁵, John R. Maben², Lynn M. Russell³, Joanna D. Kinsey^{1,6}, Inger Marie B. Tyssebotn¹, Patricia K. Quinn⁷, and Timothy S. Bates^{7,8}

¹Department of Chemistry, State University of New York, College of Environmental Science and Forestry, Syracuse, New York, USA, ²Department of Environmental Sciences, University of Virginia, Charlottesville, Virginia, USA, ³Scripps Institution of Oceanography, University of California, San Diego, La Jolla, California, USA, ⁴Now at: Department of Chemistry, University of California, Berkeley, California, USA, ⁵John A. Paulson School of Engineering and Applied Sciences, Harvard University, Cambridge, Massachusetts, USA, ⁶Now at Department of Marine Earth and Atmospheric Sciences, North Carolina State University at Raleigh, Raleigh, North Carolina, USA, ⁷Pacific Marine Environmental Laboratory, NOAA, Seattle, Washington, USA, ⁸Joint Institute for the Study of the Atmosphere and Ocean, University of Washington, Seattle, Washington, USA

Abstract The oceans hold a massive quantity of organic carbon, nearly all of which is dissolved and more than 95% is refractory, cycling through the oceans several times before complete removal. The vast reservoir of refractory dissolved organic carbon (RDOC) is a critical component of the global carbon cycle that is relevant to our understanding of fundamental marine biogeochemical processes and the role of the oceans in climate change with respect to long-term storage and sequestration of atmospheric carbon dioxide. Here we show that RDOC includes surface-active organic matter that can be incorporated into primary marine aerosol produced by bursting bubbles at the sea surface. We propose that this process will deliver RDOC from the sea surface to the atmosphere wherein its photochemical oxidation corresponds to a potentially important and hitherto unknown removal mechanism for marine RDOC.

1. Introduction

Primary marine aerosol (PMA) emitted from the ocean surface by breaking waves and bursting bubbles is highly enriched in marine organic matter (OM) relative to seawater [Keene *et al.*, 2007; Facchini *et al.*, 2008; Quinn *et al.*, 2014]. This sea-to-air flux is also the major source of aerosol mass and an important source of aerosol number (mass and number, respectively, of particles per unit volume of air) in Earth's troposphere [Andreae and Rosenfeld, 2008]. It is widely assumed that PMA OM originates from recent biological activity in the photic zone, based on correlations between field or satellite-derived chlorophyll *a* (Chl *a*) and organic carbon concentrations in ambient aerosol measured downwind of bloom regions [e.g., O'Dowd and de Leeuw, 2007; Scire *et al.*, 2009; Spracklen *et al.*, 2008; Vignati *et al.*, 2010; Fuentes *et al.*, 2011; Gantt *et al.*, 2011; Rinaldi *et al.*, 2013]. This supposition was recently challenged by Quinn *et al.* [2014] who found no positive correlation between Chl *a* and organic carbon enrichments in freshly formed PMA produced from biologically productive and oligotrophic seawater.

Long *et al.* [2014] hypothesized that at least two distinct reservoirs of organic surfactants in the ocean modulate PMA production. One reservoir is generated during the day in biologically productive waters and a second background reservoir is present in both productive and oligotrophic waters. For a given detrainment rate of bubble air, number production fluxes of PMA (number of particles produced per unit area per unit time), modulated by the background reservoir in oligotrophic waters, were statistically indistinguishable from those in biologically productive waters during late night [Long *et al.*, 2014].

Together, the Long *et al.* [2014] and Quinn *et al.* [2014] results suggest that the OM enrichment of most PMA produced globally is controlled by a large background reservoir of organic surfactants that is decoupled from OM generated by recent biological activity in the photic zone. One potential source of this background reservoir of organic surfactants is refractory dissolved organic carbon (RDOC). RDOC comprises most of the dissolved organic carbon in the oceans and has an estimated lifetime of 16,000 years [Hansell *et al.*, 2012; Hansell, 2013], cycling through the oceans several times before its complete removal [Williams and Druffel, 1987]. Little is known regarding production and removal mechanisms of RDOC. Recent findings suggest

microbial and sedimentary sources for this carbon [Guo and Santschi, 2000; Jiao *et al.*, 2010], and several removal mechanisms have been proposed [Mopper *et al.*, 1991; Lang *et al.*, 2006], although large uncertainties persist [Hansell, 2013; Repeta, 2015]. As part of the Western Atlantic Climate Study (WACS), we investigated the surface-active properties of RDOC, its incorporation into PMA, and the potential importance of its removal from the surface ocean via PMA production and atmospheric processing. Although some results generated during WACS have been reported by Quinn *et al.* [2014] and Long *et al.* [2014], all information presented herein without attribution has not been published previously.

2. Methods

PMA production from productive waters on Georges Bank, approximately 170 km east of Boston (~41.9°N, 67.4°W, Station 1), oligotrophic waters in the Sargasso Sea (~36.3°N, 64.7°W, Station 2), and North Atlantic Deep Water (NADW) sampled at a depth of 2505 m in the Sargasso Sea (~36.3°N, 64.7°W) was investigated during a cruise on the R/V *Ronald H. Brown* in the western North Atlantic Ocean from 19 to 27 August 2012 [Long *et al.*, 2014; Quinn *et al.*, 2014]. Relevant supporting data were generated using the same techniques as part of the California Nexus (CalNex) Experiment during a cruise on the R/V *Atlantis* in the eastern North Pacific Ocean off the California coast from 15 May to 6 June 2010 [Quinn *et al.*, 2014].

2.1. Marine Aerosol Generator

Model PMA (mPMA) were produced from seawater in a high-capacity generator fabricated from Pyrex and PTFE Teflon [Keene *et al.*, 2007; Long *et al.*, 2014]. The diameter of the generator was 20 cm and consisted of a 122 cm deep seawater reservoir underlying a 97 cm deep atmosphere. For characterization of mPMA produced from near-surface waters, fresh seawater from the ship's clean seawater line flowed at 4 L min^{-1} into the base of the seawater reservoir and drained evenly over the top annular rim, continuously replacing the seawater surface and minimizing formation of standing bubble rafts. For characterization of mPMA produced from NADW, approximately 200 L were collected at a depth of 2505 m in 24 Niskin bottles attached to a sampling rosette. NADW was transferred to precleaned 20 L Teflon-lined, high-density polyethylene (HDPE) carboys, allowed to warm to ambient temperature (~24°C), and pumped into the generator with a peristaltic pump configured with silicone tubing. Given the finite volume of NADW available for characterization of mPMA production, the seawater flow was reduced to 2.6 L min^{-1} thereby extending the duration of the observation period. Characterization of the generator's performance during prior deployments on Bermuda [Keene *et al.*, 2007] and at sea during CalNex [Long *et al.*, 2014] demonstrated that mPMA number production fluxes did not vary significantly over seawater flow rates through the generator ranging from 2 to 5 L min^{-1} .

For all experiments, bubble plumes were generated by pumping ultrapure air [Keene *et al.*, 2007] through either a coarse-porosity sintered glass frit (45 mm diameter, 145 to 174 μm pore size) or a bank of 11 fine-porosity sintered glass frits (90 mm diameter, 10 to 20 μm pore size) positioned at an average depth of 84 cm below the air-seawater interface. mPMA were produced when the bubbles rose to and burst at the air-seawater interface. Bubble sizes within 2 to 4 cm of the air-water interface in the aerosol generator were quantified via computer-enhanced camera images and *ImageJ* software (<http://rsb.info.nih.gov/ij/index.html>). Ultrapure air hydrated to a relative humidity (RH) of $80 \pm 2\%$ flowed at 70 L min^{-1} through the head space above the seawater reservoir. mPMA were sampled for physical and chemical characterization through isokinetic ports at the top of the generator.

For a given set of conditions, number production efficiencies (PE_{num} , number of particles produced per unit volume of air detrained in units of L^{-1}) varied as a function of frit porosities (coarse or fine) from which PMA were generated [Long *et al.*, 2014]. Since mPMA were produced from NADW using the coarse-porosity frit at a bubble flow rate of 4.4 L min^{-1} , to minimize sources of variability, results reported herein focus primarily on data for the subset of periods during which mPMA were produced from near-surface seawater using these same conditions (bubble flow rate of 4.4 L min^{-1} through the coarse frit).

Like all other models (both physical and numerical) of PMA production at the ocean surface, the aerosol generator used for this study does not perfectly mimic all aspects of PMA production in the ambient environment. Steady state void fractions (volume of bubble air in the water column divided by the volume of the water column) integrated over depth within the generator using the coarse frit (0.003 to $0.005 \text{ L}_{\text{air}} \text{ L}_{\text{sw}}^{-1}$) and fine frits (0.015 to $0.020 \text{ L}_{\text{air}} \text{ L}_{\text{sw}}^{-1}$) at typical bubble rates employed for this study fell

within or near the lower limits of reported ranges produced by breaking waves on the ocean surface (e.g., 0.03 to 0.11 $L_{\text{air}} L_w^{-1}$ at 10 cm depth [Bezzabotnov, 1985]; 0.007 to 0.065 $L_{\text{air}} L_w^{-1}$ at 30 cm depth [Deane and Stokes, 2002]) and in wave-tank experiments (0.012 to 0.37 $L_{\text{air}} L_w^{-1}$) [Rojas and Loewen, 2010]. The depth of bubble plumes within the generator also overlaps the depth range of ambient bubble clouds produced by breaking waves on the open ocean surface [Thorpe, 1982; Thorpe et al., 1982; Thorpe and Hall, 1983]. We recognize that size distributions of bubbles and associated mPMA generated by frits may be shifted somewhat toward smaller sizes relative to those produced by water jets or breaking waves [e.g., Prather et al., 2013]. However, the objective of this study was to evaluate, under controlled conditions (e.g., air-detrainment rates), variability in nascent PMA properties introduced by major physical, chemical, and biological drivers in seawater. For such studies, the physical scale, control features, and mobility of our generator provide a unique capability to examine the fundamental processes that modulate this major and as yet poorly constrained pathway in the Earth system.

2.2. Seawater Characteristics

Measurement techniques for seawater salinity, temperature, and solar radiation are reported by Long et al. [2014]. Chlorophyll *a* was quantified by filtering seawater through premuffled (550°C, 8 h) Whatman 25 mm diameter GF/F glass fiber filters and extracting the filtered Chl *a* with 90% acetone for 24 h at -20° C in the dark. Samples were analyzed using a model TD-10 AU digital fluorometer (Turner Designs). Dissolved organic carbon (DOC) was measured in seawater samples following gravity filtration through a pre-cleaned [Toole et al., 2003], 0.2 μm Whatman POLYCAP 75 AS filter capsule. DOC was quantified with a Shimadzu Model TOC-V CSH high-temperature carbon analyzer at 680°C using a combustion column containing quartz beads and platinum catalyst [Keene et al., 2007]. The chemical and physical characteristics of seawater from which mPMA were produced are summarized in supporting information Table S1.

The dynamic bubble surface tension of seawater was measured within 2 h of collection with a Sensadyne Model QC-6000 maximum bubble pressure method surface tensiometer calibrated with low-organic-carbon Type 1 deionized water (>18.3 MΩ cm, DIW) and reagent grade isopropyl alcohol as described in detail by Long et al. [2014]. Briefly, bubbles were generated using dual quartz capillary tubes, with radii of 0.25 and 2 mm, and ultrahigh purity dry air at 35 psi. Capillaries were submerged approximately 4 cm into 50 mL aliquots of unfiltered seawater samples in acid-cleaned fluorinated HDPE bottles at room temperature. The ship's motion limited measurements to bubble surface ages ranging from 0.1 to 4 s. The surface tension depression relative to water of identical salinity and temperature but devoid of surfactant material was calculated based on the Krümmel equation [Sharqawy et al., 2010].

2.3. mPMA Physical Characterization

mPMA number concentrations from 0.01 to 15 μm dry diameter in the generator head space were quantified continuously with a Scanning Electrical Mobility Spectrometer (SEMS, Brechtel Manufacturing, Inc.) and a TSI Model 3321 Aerodynamic Particle Sizer (APS) using a 5 min integration time. Measurements were processed with the manufacturer's software for standard operating conditions, and the algorithms included corrections for flow rates measured below the set point. Between 2030 and 2110 on 26 August 2012, plumbing issues resulted in the need for additional corrections and higher uncertainties. The lower sample flow resulted in a one-bin (~5 s) offset error in both upscans and downscans that was corrected by shifting the sizing bins, resulting in a <10 nm correction to the peak size [Russell et al., 1995]. Corrections were applied to remove a 0.05 V offset in the averaged SEMS sample flow rate (0.31 L min⁻¹ was corrected to recorded flow of 0.36 L min⁻¹) that was associated with electrical interference in the data acquisition board during this same period. Concentration spikes at sizes above 500 nm were recorded during this same 40 min period, likely because the instrument reached RH > 40% producing electrical arcing. Consequently, during this period, SEMS results for size bins larger than 500 nm were not used and mPMA sizes larger than 600 nm were quantified with the APS. We estimate the electrical interference caused additional uncertainty in the corrected number concentration of ±7% between 2030 and 2110 on 26 August 2012.

2.4. mPMA Chemical Characteristics

Size-resolved mPMA was sampled at 30 L min⁻¹ for chemical characterization with two nonrotating multiorifice uniform deposit impactors [Marple et al., 1991] deployed in parallel and configured with precombusted 47 mm diameter aluminum substrates and a 37 mm diameter quartz backup filter. The 50% aerodynamic cut

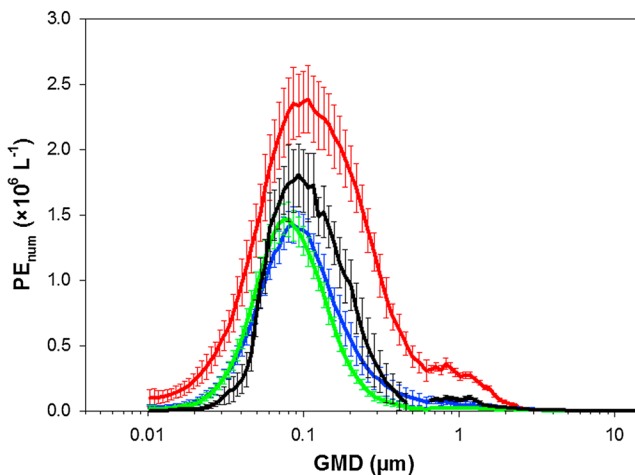


Figure 1. Average size-resolved number production efficiencies, PE_{num} , for near-surface seawater at Station 1 during the daytime (4 h following sunrise through 2 h following sunset, $n = 54$, red) and late night (6 h preceding sunrise, $n = 66$, blue), near-surface seawater at Station 2 ($n = 133$, green), and NADW ($n = 7$, black). Size-resolved PE_{num} values during daytime and nighttime at Station 2 were statistically indistinguishable [Long *et al.*, 2014] and, thus, are depicted as a single, combined distribution. n represents the number of size-resolved scans from which the average distributions were calculated; GMD refers to the dry geometric mean diameter. Errors bars depict standard deviations.

at the State University of New York, College of Environmental Science and Forestry using a Shimadzu Model TOC-V CSH carbon analyzer.

The chemical composition of mPMA was characterized and interpreted based on enrichment in organic carbon relative to seawater. The enrichment factor (EF) was calculated as the ratio of OC_{we} to Na^+ (a chemically conservative tracer of inorganic sea salt) concentrations measured in sampled mPMA divided by the corresponding ratio of DOC to Na^+ concentrations in the seawater from which the particles were produced (see Sander *et al.* [2003] for additional details regarding the calculation and interpretation of EFs).

3. Results and Discussion

Despite large differences in the contribution of RDOC to DOC in surface Sargasso Sea water relative to NADW [Hansell, 2013], the range in size-resolved PE_{num} values for NADW overlapped those for near-surface seawater sampled at Stations 1 during late night and at Station 2 (Figure 1). In contrast, average size-resolved PE_{num} values for near-surface seawater at Station 1 during the day were significantly greater (Figure 1), which is consistent with enhanced mPMA production associated with surfactants produced in biologically productive waters during the day as reported previously [Long *et al.*, 2014]. These results suggest that the reservoirs of surfactants that modulate mPMA production from oligotrophic waters, biologically productive waters at night, and NADW have similar properties. NADW DOC is primarily composed of RDOC and is essentially devoid of labile OM originating from recent biological activity and of OM associated with older semilabile and semirefractory DOC pools, whereas in the surface ocean, RDOC varies spatially and temporally from 50% to nearly 100% of DOC [Carlson, 2002; Hansell, 2013; Repeta, 2015; Carlson and Hansell, 2015]. It follows that the background reservoir of surfactants that modulates mPMA production in the surface ocean may contain RDOC.

mPMA generated from NADW and sampled in bulk was highly enriched in RDOC. The corresponding EF (133 ± 10) fell within the relatively wide range of those for mPMA OM produced from near-surface seawater during WACS summed overall size fractions (Figure S1) and from Sargasso seawater during a prior generator deployment at Bermuda (median EF 387) [Keene *et al.*, 2007]. These observations coupled with the ubiquitous presence of RDOC in the surface ocean demonstrate that PMA highly enriched in RDOC can be produced from bursting bubbles at the ocean surface.

diameters for the impactor stages were 18, 10, 5.6, 3.2, 1.8, 1.0, 0.56, 0.32, and $0.18\text{ }\mu\text{m}$ diameter at the RH of the generator head space. mPMA was also sampled in bulk (upper size limit of approximately $20\text{ }\mu\text{m}$ diameter at the RH within the head space) [Keene *et al.*, 2007] at 30 L min^{-1} on two precombusted 47 mm diameter quartz filters deployed in parallel. Size-resolved and bulk samples for analysis of Na^+ (and other inorganic ions) were transferred to precleaned 10 mL HDPE tubes and stored at -20°C . Samples were extracted in 5 mL of DIW and analyzed by high-performance ion chromatography at the University of Virginia. Size-segregated and bulk samples for analysis of water-extractable OC (OC_{we}) [Keene *et al.*, 2007] were transferred to precombusted 10 mL Pyrex centrifuge tubes, extracted immediately with 5 mL DIW, stored at -20°C , and analyzed

mPMA number production fluxes from surface seawater are dominated by particles with dry diameters in the range of 60 to 90 nm and nonwater masses mainly comprised of OM [Keene *et al.*, 2007; Facchini *et al.*, 2008; Quinn *et al.*, 2014]. The finite sample volume of NADW limited the duration of associated PMA production, and consequently, the sampled aerosol mass was insufficient for reliable quantification of size-resolved EFs. However, EFs for mPMA produced from the surface ocean increased with decreasing size to substantially higher values ranging from 10^4 to 10^6 for the smallest size fraction (Figure S1). The high EF for bulk mPMA produced from NADW coupled with the size-resolved EFs for mPMA produced from near-surface seawater (Figure S1) and the similarity among size-resolved PE_{num} values for NADW and near-surface waters in both oligotrophic regions and biologically productive regions at night (Figure 1) implies that the size-resolved EFs for mPMA produced from all water types including NADW will also be similar, supporting the hypothesis that OM in the form of RDOC is a major component of submicron PMA emitted from the NADW.

Organic matter decreases the surface tension at interfaces including bubble surfaces, and the magnitude of this decrease varies as a function of the composition and quantity of OM present and interface age [Shargawy *et al.*, 2010]. The average decrease in the dynamic bubble surface tension at a mean surface age of 2.2 s measured during aeration of NADW was $1.1 \pm 0.2 \text{ mN m}^{-1}$ indicating that surface-active OM associated with RDOC in NADW was present at concentrations sufficient to quickly (seconds) coat bubble surfaces. As a reference, the surface tension of surfactant-free seawater at 35.00 ppt is 72.99 mN m^{-1} at 25°C. The decrease in the bubble surface tension for NADW was within the range of those for surface waters during WACS (0.4 to 1.2 mN m^{-1}) [Long *et al.*, 2014]. The similarity in surfactant activity associated with RDOC in NADW and with OM in surface waters implies that RDOC in surface waters contributes to the background reservoir of surfactants that coat bubbles in the surface ocean and to the PMA OM produced when those bubbles burst at the sea surface.

Differences in OM-mediated surface tensions among the different water types also contributed to variability in the corresponding bubble volume distributions (Table S1). The Mann-Whitney test indicates that the bubble volume distributions in biologically productive waters at Station 1 differed significantly from those in oligotrophic waters at Station 2 ($p < 0.001$) and in the NADW ($p < 0.001$). The relatively smaller bubble volumes at Station 1 are consistent with expectations for influences on bubble size of surfactants that were produced during daytime in biologically productive waters (see Long *et al.* [2014] for additional details regarding the effect of surfactant OM on bubble volumes). Although bubble volume distributions for Station 2 and in the NADW did not differ significantly ($p = 0.297$), the wider range for Station 2 (Table S1) reflects a relatively small number (~15%) of bubbles volumes that were greater than the range of those in the NADW. These results imply that bubble plume dynamics in near-surface oligotrophic waters and in NADW are controlled by reservoirs of surfactant OM that have similar although not identical properties. Taken together, the above results support the hypothesis that the background reservoir of organic surfactants in the surface ocean that modulates PMA production and the associated emission of particulate OM to the atmosphere is partly comprised of RDOC.

Our results have important implications not only for understanding sources, composition, and influences of particulate OM in the marine atmosphere but also for the cycling of RDOC in the oceans. Once injected into the atmosphere in association with PMA, RDOC is expected to undergo photochemical oxidation over the lifetime of the aerosol, which for submicron-diameter size fractions ranges from several days to a week or more [Warneck, 2000]. Since RDOC is photoreactive in seawater [Mopper *et al.*, 1991], it is expected to also be photoreactive in PMA but at rates that are greatly amplified owing to acidic conditions ($\text{pH} \approx 2$ to 5) [Keene *et al.*, 2002; Pszenny *et al.*, 2004] and to the presence of three to ten orders of magnitude higher aqueous-phase concentrations of oxidants including the OH radical, hydrogen peroxide ($100 \mu\text{M}$, based on a Henry's Law constant of $1 \times 10^5 \text{ M atm}^{-1}$ and an average marine tropospheric concentration of 1 ppbv [Jackson and Hewitt, 1999]), nitrate ion (e.g., $\sim 0.4 \text{ M } \text{NO}_3^-$) [Keene *et al.*, 2002], and ozone. Zhou *et al.* [2008] measured midday rates of photochemical formation of the OH radical and hydroperoxides in mPMA produced from surface Sargasso seawater that were factors of 10^3 to 10^4 higher than production rates in seawater.

Photochemical processing and chemical evolution of PMA in response to rapid acidification (seconds to minutes) [Chameides and Stelson, 1992; Erickson *et al.*, 1999], exposure to full spectral solar radiation, and production and incorporation of photochemically reactive oxidants including the nitrate ion [Prospero and Savoie, 1989] will

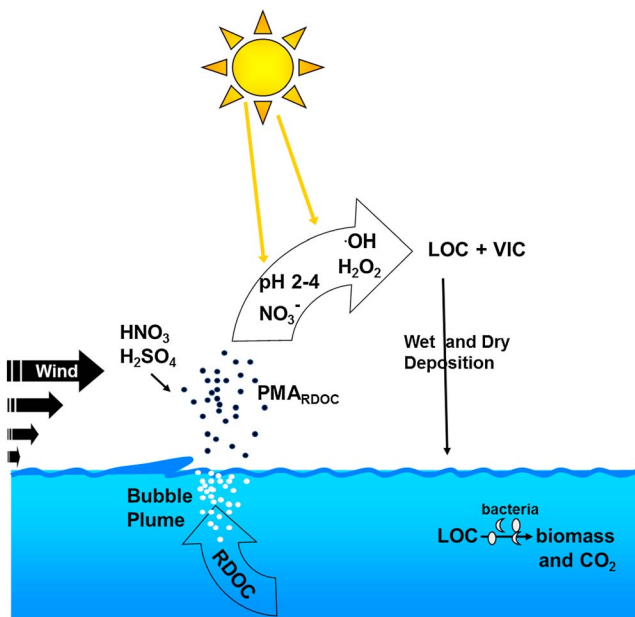


Figure 2. Conceptual model for the loss of RDOC through adsorption onto rising bubbles that burst at the sea surface injecting RDOC into the troposphere in association with PMA. Rapid adsorption of inorganic and organic acids from the gas phase will acidify PMA within minutes of production from an initial pH of approximately 8 to pHs typically in the range of 2 to 4 [Chameides and Stelson, 1992; Erickson et al., 1999]. PMA will also become highly oxidizing through the in situ photochemical production and adsorption of reactive species including hydrogen peroxide, ozone, reactive halogens, and the OH radical [Zhou et al., 2008]. In acidic and highly oxidizing PMA, RDOC reacts to form volatile inorganic carbon (VIC) products including CO and CO₂, and low molecular weight organic-carbon (LOC) products including aldehydes, ketones, and organic acids. LOC products that deposit back into the sea via wet and dry deposition will be readily assimilated and respired by the marine food web.

Table 1. Estimated Residence Time of RDOC^a Based on Several Published Estimates for the Global Production Flux of PMA OM and the Fractional Contribution of RDOC to the PMA OM Flux^b

Flux (Tg C yr ⁻¹)	Fraction of RDOC Associated With PMA OM Flux	$\tau_{\text{sea-air}} (\text{yr})^c$
29 ^d	0.1	220,000
	0.5	43,000
	1.0	22,000
22.3 ^e	1.0	28,000
35–50 ^f	1.0	13,000–18,000
8 ^g	1.0	79,000

^aResidence time calculation implicitly assumes RDOC steady state, which is a reasonable assumption for the proof of concept calculation done here. However, RDOC production rates and losses are poorly constrained and RDOC may not be in steady state.

^bThese calculations assume that RDOC is oxidized in the atmosphere to forming products that are not recalcitrant.

^c $\tau_{\text{sea-air}}$ is the residence time equal to the total RDOC reservoir in the oceans (630 Pg C) [Hansell, 2013] divided by the flux of PMA OM into the atmosphere times the fractional contribution of RDOC to the OM flux.

^d[Long et al., 2011].

^e[Gantt et al., 2009].

^f[Roelofs, 2008].

^g[Spracklen et al., 2008].

markedly modify the organic composition, resulting in the formation of reaction products including volatile inorganic species (CO and CO₂) and low-molecular-weight organic compounds (e.g., acetone and carboxylic acids) (Figure 2). Therefore, it is reasonable to assume that at low pH and under highly oxidizing atmospheric conditions in the presence of sunlight, some fraction of PMA RDOC will be photochemically oxidized over the atmospheric lifetime of the aerosol, particularly in the longer-lived submicron-diameter size fractions with which 70 to 80% of PMA OM is typically associated [Keene et al., 2007; Facchini et al., 2008; Quinn et al., 2014].

To evaluate the potential importance of this pathway, we calculated a range in residence times for marine RDOC in response to atmospheric processing based on (1) several published estimates for the global production flux of OM associated with PMA at the sea surface that span the range of published fluxes and (2) a range in fractional contributions of RDOC to the PMA OM flux (Table 1). If global PMA OM emissions fall within the middle to upper end of the range in published estimates and most PMA OM is comprised of RDOC that is subsequently oxidized in the atmosphere, then the range of residence times for marine RDOC due to this coupled ocean-atmosphere process would be comparable to the estimated 12,700 to 13,300 years residence time of RDOC in the oceans based on a reservoir size of 630 ± 32 Pg and a loss rate of $0.003 \mu\text{mol C kg}^{-1} \text{yr}^{-1}$ [Hansell, 2013]. However, this is considered an upper limit since some RDOC is undoubtedly processed in the oceans [Repeta, 2015]. A more likely scenario is that RDOC comprises a smaller fraction of PMA OM that is roughly proportional to its fractional contribution to OM in the surface mixed layer [Hansell, 2013],

and only a portion of the RDOC is oxidized in the atmosphere to form volatile or biologically labile products. In this case, atmospheric processing would result in a longer residence time and constitute a smaller but potentially still significant fraction of RDOC loss, as noted in Table 1. Several outstanding questions must be addressed to resolve the overall importance of this pathway as a removal mechanism for RDOC: (1) what is the global production flux of PMA OM, (2) what is the fractional contribution of RDOC to the PMA OM production flux, and (3) what fraction of RDOC is oxidized in the atmospheric over the lifetime of the aerosol and thereby removed by this process? Question one will be perhaps the most difficult to resolve, since reported fluxes vary nearly an order of magnitude and the major factors that modulate PMA OM emissions are highly uncertain.

In conclusion, our results suggest that the largest reservoir of dissolved OM in the oceans, RDOC, includes surface-active constituents that associate with bubble surfaces produced by wind waves thereby modulating surface tension, bubble plume dynamics, PMA production, and PMA composition. Findings reported herein together with previous measurements of mPMA EFs and the photochemical evolution of associated OM by our group and others support the hypothesis that removal of RDOC from the oceans via PMA production and its subsequent oxidation in the atmosphere is a potentially important recycling mechanism for marine RDOC. Oxidized organic reaction products would include formic, acetic, and oxalic acids that are ubiquitous gas- and particulate-phase chemical constituents of marine air [Turekian *et al.*, 2003; Keene *et al.*, 2015]. Indeed, significant production of short-lived organic reaction products via this pathway could help account for the high concentrations of carboxylic acids [Keene *et al.*, 2015] and glyoxal [Sinreich *et al.*, 2010] over the remote ocean that are difficult to reconcile with known sources of marine-derived organic precursors. Although this work focused on carbon, the proposed ocean-atmosphere coupled pathway may also represent an important mechanism whereby recalcitrant forms of marine nitrogen [Aluwihare *et al.*, 2005] are recycled in the atmosphere and subsequently resupplied to the oceans in nutrient forms via wet and dry deposition.

Acknowledgments

Data and analyses reported in this study are available upon request from the authors. We thank G. Henderson, D. Coffman, K. Schulz, D. Hamilton, J. Johnson, and M. Haserodt for their assistance in sample collection and analysis; V. Trainer for the loan and calibration of the fluorometer; X. Lopez-Yglesias and F. Brechtel of Brechtel Manufacturing for their timely assistance with data inversions; and the captains and crews of the NOAA R/V *Ronald H. Brown* and the UNOLS R/V *Atlantis* for logistical support; and to three anonymous reviewers for their constructive comments that improved this manuscript. Financial support for this work was provided by the National Science Foundation through awards to the State University of New York, College of Environmental Science and Forestry (OCE-0948216 and OCE-1129896), University of Virginia (OCE-0948420 and OCE-1129836), Scripps Institution of Oceanography (OCE-1129580), and Harvard University (AGS-1252755). Additional support was provided by the NOAA Atmospheric Composition and Climate Program.

References

- Aluwihare, L. I., D. J. Repeta, S. Pantoja, and C. G. Johnson (2005), Two chemically distinct pools of organic nitrogen accumulate in the ocean, *Science*, 308(5724), 1007–1010, doi:10.1126/science.1108925.
- Andreae, M. O., and D. Rosenfeld (2008), Aerosol-cloud-precipitation interactions. Part 1. The nature and sources of cloud-active aerosols, *Earth Sci. Rev.*, 89(1–2), 13–41, doi:10.1016/j.earscirev.2008.03.001.
- Bezzabotnov, V. S. (1985), Certain results of field measurements of the structure of sea-foam formation, *Izv. Atmos. Oceanic Phys.*, 21(1), 77–79.
- Carlson, C. A. (2002), Production and removal processes, in *Biogeochemistry of Marine Dissolved Organic Matter*, edited by D. A. Hansell and C. A. Carlson, Academic Press, New York.
- Carlson, C. A., and D. A. Hansell (2015), DOM sources, sinks, reactivity, and budgets, in *Biogeochemistry of Marine Dissolved Organic Matter*, 2nd ed., edited by D. A. Hansell and C. A. Carlson, Academic Press, New York.
- Chameides, W. L., and A. W. Stelson (1992), Aqueous-phase chemical processes in deliquescent sea salt aerosols: A mechanism that couples the atmospheric cycles of S and sea salt, *J. Geophys. Res.*, 97(D18), 20,565–20,580, doi:10.1029/92JD01923.
- Deane, G. B., and M. D. Stokes (2002), Scale dependence of bubble creation mechanisms in breaking waves, *Nature*, 418(6900), 839–844, doi:10.1038/nature00967.
- Erickson, D. J., C. Seuzaret, W. C. Keene, and S. L. Gong (1999), A general circulation model based calculation of HCl and ClNO₂ production from sea-salt dechlorination: Reactive Chlorine Emissions Inventory, *J. Geophys. Res.*, 104(D7), 8347–8372, doi:10.1029/98JD01384.
- Facchini, M. C., et al. (2008), Primary submicron marine aerosol dominated by insoluble organic colloids and aggregates, *Geophys. Res. Lett.*, 35, L17814, doi:10.1029/2008GL034210.
- Fuentes, E., H. Coe, D. Green, and G. McFiggans (2011), On the impacts of phytoplankton-derived organic matter on the properties of primary marine aerosol—Part 2: Composition, hygroscopicity and cloud condensation activity, *Atmos. Chem. Phys.*, 11(6), 2585–2602, doi:10.5194/acp-11-2585-2011.
- Gantt, B., N. Meskhidze, and D. Kamkowsky (2009), A new physically-based quantification of marine isoprene and primary organic aerosol emissions, *Atmos. Chem. Phys.*, 9(14), 4915–4927, doi:10.5194/acp-9-4915-2009.
- Gantt, B., N. Meskhidze, M. C. Facchini, M. Rinaldi, D. Ceburnis, and C. D. O'Dowd (2011), Wind speed dependent size-resolved parameterization for the organic mass fraction of sea spray aerosol, *Atmos. Chem. Phys.*, 11(16), 8777–8790, doi:10.5194/acp-11-8777-2011.
- Guo, L., and P. H. Santschi (2000), Sedimentary sources of old high molecular weight dissolved organic carbon from the ocean margin benthic nepheloid layer, *Geochim. Cosmochim. Acta*, 64(4), 651–660, doi:10.1016/S0016-7037(99)00335-X.
- Hansell, D. A. (2013), Recalcitrant dissolved organic carbon fractions, *Annu. Rev. Mar. Sci.*, 5, 421–445, doi:10.1146/annurev-marine-120710-100757.
- Hansell, D. A., C. A. Carlson, and R. Schlitzer (2012), Net removal of major marine dissolved organic carbon fractions in the subsurface ocean, *Global Biogeochem. Cycles*, 26, GB1016, doi:10.1029/2011GB004069.
- Jackson, A. V., and C. N. Hewitt (1999), Atmosphere hydrogen peroxide and organic hydroperoxides: A review, *Crit. Rev. Environ. Sci. Technol.*, 29(2), 175–228, doi:10.1080/1064338991259209.
- Jiao, N., et al. (2010), Microbial production of recalcitrant dissolved organic matter: Long-term carbon storage in the global ocean, *Nat. Rev. Microbiol.*, 8(8), 593–599, doi:10.1038/nrmicro2386.
- Keene, W. C., A. A. P. Pszenny, J. R. Maben, and R. Sander (2002), Variation of marine aerosol acidity with particle size, *Geophys. Res. Lett.*, 29(7), 1101, doi:10.1029/2001GL013881.
- Keene, W. C., et al. (2007), Chemical and physical characteristics of nascent aerosols produced by bursting bubbles at a model air-sea interface, *J. Geophys. Res.*, 112, D21202, doi:10.1029/2007JD008464.

- Keene, W. C., J. N. Galloway, G. E. Likens, F. A. Deviney, K. N. Mikkelsen, J. L. Moody, and J. R. Maben (2015), Atmospheric wet deposition in remote regions: Benchmarks for environmental change, *J. Atmos. Sci.*, 72(8), 2947–2978, doi:10.1175/JAS-D-14-0378.
- Lang, S. Q., D. A. Butterfield, M. D. Lilley, H. P. Johnson, and J. I. Hedges (2006), Dissolved organic carbon in ridge-axis and ridge-flank hydrothermal systems, *Geochim. Cosmochim. Acta*, 70(15), 3830–3842, doi:10.1016/j.gca.2006.04.031.
- Long, M. S., W. C. Keene, D. J. Kieber, D. J. Erickson, and H. Maring (2011), A sea-state based source function for size- and composition-resolved marine aerosol production, *Atmos. Chem. Phys.*, 11(3), 1203–1216, doi:10.5194/acp-11-1203-2011.
- Long, M. S., et al. (2014), Light-enhanced primary marine aerosol production from biologically productive seawater, *Geophys. Res. Lett.*, 41, 2661–2670, doi:10.1002/2014GL059436.
- Marple, V. A., K. L. Rubow, and S. M. Behm (1991), A microifice uniform deposit impactor (MOUDI): Description, calibration, and use, *Aerosol Sci. Technol.*, 14(4), 434–446, doi:10.1080/02786829108959504.
- Mopper, K., et al. (1991), Photochemical degradation of dissolved organic carbon and its impact on the oceanic carbon cycle, *Nature*, 353(6339), 60–62, doi:10.1038/353060a0.
- O'Dowd, C. D., and G. de Leeuw (2007), Marine aerosol production: A review of the current knowledge, *Philos. Trans. R. Soc. London, Ser. A*, 365(1856), 1753–1774, doi:10.1098/rsta.2007.2043.
- Prather, K. A., et al. (2013), Bringing the ocean into the laboratory to probe the chemical complexity of sea spray aerosol, *Proc. Natl. Acad. Sci. U.S.A.*, 110(19), 7550–7555, doi:10.1073/pnas.1300262110.
- Prospero, J. M., and D. L. Savoie (1989), Effect of continental sources on nitrate concentrations over the Pacific Ocean, *Nature*, 339(6227), 687–689, doi:10.1038/339687a0.
- Pszenny, A. A. P., J. Moldanová, W. C. Keene, R. Sander, J. R. Maben, M. Martinez, P. J. Crutzen, D. Perner, and R. G. Prinn (2004), Halogen cycling and aerosol pH in the Hawaiian marine boundary layer, *Atmos. Chem. Phys.*, 4(1), 147–168, doi:10.5194/acp-4-147-2004.
- Quinn, P. K., T. S. Bates, K. S. Schulz, D. J. Coffman, A. A. Frossard, L. M. Russell, W. C. Keene, and D. J. Kieber (2014), Contribution of sea surface carbon pool to organic matter enrichment in sea spray aerosol, *Nat. Geosci.*, 7, 228–232, doi:10.1038/ngeo2092.
- Repeta, D. J. (2015), Chemical characterization and cycling of dissolved organic matter, in *Biogeochemistry of Marine Dissolved Organic Matter*, 2nd ed., edited by D. A. Hansell and C. A. Carlson, Academic Press, New York.
- Rinaldi, M., et al. (2013), Is chlorophyll- α the best surrogate for organic matter enrichment in submicron primary marine aerosol?, *J. Geophys. Res. Atmos.*, 118, 4964–4973, doi:10.1002/jgrd.50417.
- Roelofs, G. J. (2008), A GCM study of organic matter in marine aerosol and its potential contribution to cloud drop activation, *Atmos. Chem. Phys.*, 8(3), 709–719, doi:10.5194/acp-8-709-2008.
- Rojas, G., and M. R. Loewen (2010), Void fraction measurements beneath plunging and spilling breaking waves, *J. Geophys. Res.*, 115, C08001, doi:10.1029/2009JC005614.
- Russell, L. M., R. C. Flagan, and J. H. Seinfeld (1995), Asymmetric instrument response resulting from mixing effects in accelerated DMA-CPA measurements, *Aerosol Sci. Technol.*, 23(4), 491–509, doi:10.1080/02786829508965332.
- Sander, R., et al. (2003), Inorganic bromine in the marine boundary layer: A critical review, *Atmos. Chem. Phys.*, 3(5), 1301–1336, doi:10.5194/acp-3-1301-2003.
- Sciare, J., et al. (2009), Long-term observations of carbonaceous aerosol in the Austral Ocean atmosphere: Evidence of a biogenic marine organic source, *J. Geophys. Res.*, 114, D15302, doi:10.1029/2009JD011998.
- Sharqawy, M. H., J. H. Lienhard, and S. M. Zubair (2010), Thermophysical properties of seawater: A review of existing correlations and data, *Desalin. Water Treat.*, 16(1–3), 354–380, doi:10.5004/dwt.2010.1079.
- Sinreich, R., S. Coburn, B. Dix, and R. Volkamer (2010), Ship-based detection of glyoxal over the remote tropical Pacific Ocean, *Atmos. Chem. Phys.*, 10(23), 11,359–11,371, doi:10.5194/acp-10-11359-2010.
- Spracklen, D. V., S. R. Arnold, J. Sciare, K. S. Carslaw, and C. Pio (2008), Globally significant oceanic source of organic carbon aerosol, *Geophys. Res. Lett.*, 35, L12811, doi:10.1029/2008GL033359.
- Thorpe, S. A. (1982), On the clouds of bubbles formed by breaking wind-waves in deep water, and their role in air-sea gas transfer, *Philos. Trans. R. Soc. London, Ser. A*, 304(1483), 155–210, doi:10.1098/rsta.1982.0011.
- Thorpe, S. A., and A. J. Hall (1983), The characteristics of breaking waves, bubble clouds, and near-surface currents observed using side-scan sonar, *Cont. Shelf Res.*, 1(4), 353–384, doi:10.1016/0278-4343(83)90003-1.
- Thorpe, S. A., A. R. Stubbs, A. J. Hall, and R. J. Turner (1982), Wave-produced bubbles observed by side-scan sonar, *Nature*, 296(5858), 636–638, doi:10.1038/296636a0.
- Toole, D. A., D. J. Kieber, R. P. Kiene, D. A. Siegel, and N. B. Nelson (2003), Photolysis and the dimethylsulfide (DMS) summer paradox in the Sargasso Sea, *Limnol. Oceanogr.*, 48(3), 1088–1100, doi:10.4319/lo.2003.48.3.1088.
- Turekian, V. C., S. A. Macko, and W. C. Keene (2003), Concentrations, isotopic compositions, and sources of size-resolved, particulate organic carbon and oxalate in near-surface marine air at Bermuda during spring, *J. Geophys. Res.*, 108(D5), 4157, doi:10.1029/2002JD002053.
- Vignati, E., M. C. Facchini, M. Rinaldi, C. Scannell, D. Ceburnis, J. Sciare, M. Kanakidou, S. Myriokefalitakis, F. Dentener, and C. D. O'Dowd (2010), Global scale emission and distribution of sea-spray aerosol: Sea-salt and organic enrichment, *Atmos. Environ.*, 44(5), 670–677, doi:10.1016/j.atmosenv.2009.11.013.
- Warneck, P. (2000), *Chemistry of the Natural Atmosphere*, 2nd ed., Academic Press, New York.
- Williams, P. M., and E. R. M. Druffel (1987), Radiocarbon in dissolved organic matter in the central North Pacific Ocean, *Nature*, 330(6145), 246–248, doi:10.1038/330246a0.
- Zhou, X., A. J. Davis, D. J. Kieber, W. C. Keene, J. R. Maben, H. Maring, E. E. Dahl, M. A. Izaguirre, R. Sander, and L. Smoydzyn (2008), Photochemical production of hydroxyl radical and hydroperoxides in water extracts of nascent marine aerosols produced by bursting bubbles from Sargasso seawater, *Geophys. Res. Lett.*, 35, L20803, doi:10.1029/2008GL035418.